TISSUE ENGINEERING: Part C
Volume 20, Number 7, 2014

DOI: 10.1089/ten.tec.2013.0446

A Human *In Vitro* Model That Mimics the Renal Proximal Tubule

Anke Hoppensack, PhD, MSc,[1,2] Christian C. Kazanecki, PhD,[3] David Colter, PhD,[4] Anna Gosiewska, PhD,[5] Johanna Schanz, PhD,[1] Heike Walles, PhD,[2,6] and Katja Schenke-Layland, PhD, MSc[1,7,8]

Human *in vitro*-manufactured tissue and organ models can serve as powerful enabling tools for the exploration of fundamental questions regarding cell, matrix, and developmental biology in addition to the study of drug delivery dynamics and kinetics. To date, the development of a human model of the renal proximal tubule (PT) has been hindered by the lack of an appropriate cell source and scaffolds that allow epithelial monolayer formation and maintenance. Using extracellular matrices or matrix proteins, an *in vivo*-mimicking environment can be created that allows epithelial cells to exhibit their typical phenotype and functionality. Here, we describe an *in vitro*-engineered PT model. We isolated highly proliferative cells from cadaveric human kidneys (human kidney-derived cells [hKDCs]), which express markers that are associated with renal progenitor cells. Seeded on small intestinal submucosa (SIS), hKDCs formed a confluent monolayer and displayed the typical phenotype of PT epithelial cells. PT markers, including N-cadherin, were detected throughout the hKDC culture on the SIS, whereas markers of later tubule segments were weak (E-cadherin) or not (aquaporin-2) expressed. Basement membrane and microvilli formation demonstrated a strong polarization. We conclude that the combination of hKDCs and SIS is a suitable cell-scaffold composite to mimic the human PT *in vitro*.

Introduction

The proximal tubule (PT) of the kidney represents the first segment of the renal tubule following the glomerular filter where the blood is filtered. Morphologically, the PT is composed of a single-layered epithelium of polarized cuboidal cells that are attached to a basement membrane.[1] Renal proximal tubule epithelial cells (RPTECs) have an apical–basal polarity with a well-developed microvilli brush border on the apical side.[1] RPTECs reabsorb most of the substances that need to be recovered from the glomerular filtrate, such as water, glucose, amino acids, and electrolytes. They also secrete waste products and xenobiotics into the tubule lumen for excretion and express several xenobiotic metabolizing enzymes.[2]

To study physiological and pathophysiological processes related to the PT epithelium, appropriate *in vitro* test models are of high interest. Drugs and their metabolites can be intensively absorbed by the numerous different transport systems of RPTECs. Therefore, renal PT-mimicking *in vitro* test systems are of particular interest for pharmacological research, since the PT epithelium influences bioavailability and is particularly sensitive toward the nephrotoxic effects of xenobiotics.[3]

The development of suitable renal cell-scaffold combinations is also of great interest to the field of bioartificial kidney (BAK) assist device design. In BAKs, renal epithelial cells are added to the conventional hemodialysis filter that can only partially replace glomerular filtration.[4–7] The outcome of most BAK *in vitro*-engineering approaches

[1]Department of Cell and Tissue Engineering, Fraunhofer Institute for Interfacial Engineering and Biotechnology (IGB), Stuttgart, Germany.
[2]Institute of Tissue Engineering and Regenerative Medicine, University Hospital of the Julius-Maximilians University, Würzburg, Germany.
[3]Janssen Diagnostics, Inc., Raritan, New Jersey.
[4]Janssen Research & Development, LLC, Janssen Pharmaceutical Companies of Johnson & Johnson, Springhouse, Pennsylvania.
[5]Johnson & Johnson Consumer and Personal Products Worldwide, Skillman, New Jersey.
[6]Oncology Project Group, Fraunhofer IGB, Würzburg, Germany.
[7]University Women's Hospital, Eberhard Karls University Tübingen, Tübingen, Germany.
[8]Cardiovascular Research Laboratories, Department of Medicine/Cardiology, David Geffen School of Medicine at UCLA, Los Angeles, California.

crucially depends on the appropriate choice of cells, substrates, and culture conditions. As one essential parameter for cell attachment and the formation and maintenance of an epithelial monolayer, the important role of the extracellular matrix (ECM) has been acknowledged and intensively investigated over the past years.[8–10] It has been shown that components of the basement membrane, such as laminins and collagen type IV (Col IV) are especially suitable coatings for the improvement of renal tubule cell attachment on synthetic polymer surfaces, which is necessary for the establishment of bioartificial renal tubules.[11] However, it has been shown that different types of renal cells prefer various ECM proteins, ECM protein concentrations, and cell culture conditions,[12,13] demonstrating the complexity of interactions between renal cells and the ECM, and the individuality of each cell and scaffold component. In addition, the utilization of hydrogels composed of collagen type I (Col I), matrigel, and bioactivated synthetic polymers for the establishment of *in vitro* cultures further illustrates the important impact that ECM proteins have on renal tubule cell morphology and functionality.[14–18] Embedded in these three-dimensional (3D) matrices, Madin-Darby canine kidney cells formed polarized cysts and tubule-like structures with an epithelial phenotype.[18] In this study, it was emphasized that the presence of at least one ECM component is crucial for cyst formation.[18] Further, it was shown that isolated PTs retain their phenotype and functions for a prolonged time in hyaluronic acid-based hydrogels.[19] Hydrogel cultures are appropriate for studying epithelial cell morphogenesis and polarization *in vitro*; however, for renal tubule cell transport function studies, these cultures are not useful since tubule structures are diffusely distributed within the gel. To date, porous well inserts are used for these functional tests since they allow planar monolayer growth with separated basolateral and apical compartments.[20] In addition, synthetic insert membranes can be coated with Col I; however, they do not mimic a true 3D environment that is capable of promoting epithelial cell monolayer formation and polarization.

Here, we present an approach using small intestinal submucosa (SIS) as a natural scaffold, which is derived from porcine small intestine.[21–23] SIS has been intensively studied in preclinical and clinical studies that revealed its benefit as a biomaterial graft to support tissue regeneration for several applications such as hernia repair[24] and urologic reconstruction.[25] SIS is prepared by removing the mucosal and muscular layers and all remaining cells to obtain a natural ECM scaffold that is mainly composed of collagens including Col I and collagen type III (Col III).[26–31] SIS supports cell ingrowth, proliferation, and differentiation, and cell phenotype maintenance of various cell types.[21,32–34] To our knowledge, SIS has not been used for the culture of renal tubule cells.

Cell source is another important factor for the success and quality of tissue cultures. In past years, research efforts have been focused on clarifying the origin and identity of cells that can contribute to the process of renal tubule regeneration.[35–37] Such endogenous stem or progenitor cells could be a useful cell source since they possess an extended proliferative potential, which is in great contrast to mature primary kidney cells.[38] They may also exhibit higher functionality under appropriate culture conditions when compared to cancerous or virally immortalized cell lines, which are routinely used in *in vitro* test systems. Here, we have isolated and characterized cells from cadaveric human kidneys (human kidney-derived cells [hKDCs]) with the focus on cell morphology, growth potential, surface marker expression, and tubulogenic differentiation. The combination of hKDCs and SIS allowed for the establishment of an *in vitro* model that mimics the renal PT.

Materials and Methods

hKDC isolation

Tissue considered unsuitable for transplantation was obtained through the National Disease Research Interchange (Philadelphia, PA) following institutional protocol approvals. To remove blood cells and debris, kidneys were washed in Dulbecco's modified Eagle's medium (DMEM, #11885-076; Life Technologies, Carlsbad, CA). Tissues were dissected from the cortex region of the kidneys. The tissues were then mechanically dissociated in tissue culture plates and digested in good manufacturing practice grade enzyme mixtures containing 0.25 units 4-phenylazobenzyloxycarbonyl activity/mL collagenase (NB6, #17452.01; Serva Electrophoresis GmbH, Heidelberg, Germany) and 2.5 units/mL dispase II (#04942078001; Roche Diagnostics Corporation, Indianapolis, IN). The enzyme mixture was combined with renal epithelial growth medium (REGM, #CC-3190; Lonza, Walkersville, CA). The conical tubes containing the tissue, medium, and digestion enzymes were incubated at 37°C in an orbital shaker at 225 rpm for 2 h. If large pieces of tissue were still present after the digestion step, they were removed by gravity sedimentation or by slow centrifugation. The supernatant that contained the suspended cells was then transferred into a new 50 mL tube and centrifuged. The cells were resuspended in REGM, plated on gelatin-coated tissue culture flasks, and cultured at 37°C under normal atmospheric conditions for cytological analyses.

Flow cytometry

Cells were expanded with REGM in cell culture flasks at 37°C and 5% CO_2. Adherent cells were washed in phosphate-buffered saline (PBS) and detached with TrypLE Select (#12563-029; Life Technologies). Cells were harvested, washed, counted, centrifuged, and resuspended in PBS containing 3% FBS at a concentration of 5×10^5 cells/mL. Antibody staining was performed using 50,000 cells according to the manufacturer's instructions (all BD Biosciences, San Jose, CA). The following antibodies were used: anti-CD13 (#347837), anti-CD24 (#555428), anti-CD29 (#555443), anti-CD34 (#555478), anti-CD44 (#555821) and anti-CD73 (#550257), IgG-FITC control antibody (#340755), and IgG-PE control antibody (#340761). Antibody staining was analyzed using a Guava EasyCyte Instrument (Guava Technologies/Millipore, Billerica, MA).

HK-2 culture

The human PT epithelial cell line HK-2, immortalized through transduction with human papillomavirus type 16 E6/E7 genes,[39] was obtained from the American Type Culture Collection (ATCC, #CRL-2190™). Cells were

seeded and expanded in cell culture flasks in REGM (#CC-3190; Lonza, Basel, Switzerland) at 37°C in a 5% CO_2 atmosphere until seeding for SIS experiments.

SIS preparation

SIS was prepared from porcine jejunal segments. All explantations were in compliance with the German Animal Protection Laws (§4 Abs. 3) and the institute's animal protection officer regularly communicated with the responsible authorities. After jejunum explantation, the mesentery was discarded, the jejunal segments were rinsed with tap water, and the mucosa was mechanically removed. All remaining cells were lysed by incubation in 3.4% sodium desoxycholate (#3484; Carl Roth, Karlsruhe, Germany). Subsequent to several washing steps in PBS at 4°C, the scaffold was sterilized by gamma irradiation (25 kGray) prior further use.

Cell culture in vitro *models*

For controls, hKDCs were seeded at a density of 1.3–5.3×10^3 cells/cm^2 in REGM in 24-well routine polystyrene cell culture plates. hKDCs were also seeded onto Col I-coated, porous polyethylene terephthalate (PET) membrane inserts in 12-well cell culture plates.[40] The Col I-coated PET membranes were seeded using 6.5×10^3 hKDCs/cm^2 in REGM. In addition, 3D Col I-composed gel cultures (Col I-3D-gels) were performed in 24-well cell culture plates. Each well was coated with 500 µL Col I gel solution consisting of 3 mg/mL Col I in DMEM (#42400-010; Life Technologies, Darmstadt, Germany) containing 30 mM HEPES (#9105; Carl Roth), 10% FCS (#10270-106; Life Technologies), and 1% gentamycin (#15710-049; Life Technologies). The solution gelled during incubation for 15 min at 37°C in REGM. For cell seeding, the medium was removed and 6.5–32.5×10^3 cells/cm^2 were seeded in REGM. After 24 h, the medium was aspirated and 300 µL of the Col I-containing gel solution (prepared as described above) was added to each cell-containing well. The collagen solution gelled during 15 min at 37°C. Finally, the gels were covered with REGM and cultured at 37°C, 5% CO_2.

For 3D SIS cultures, SIS pieces were laterally cut and opened. Single-layer SIS pieces were stretched between two stainless steel rings. Subsequently, they were transferred to 12-well cell culture plates and incubated in REGM for at least 2 h at 37°C. Medium was aspirated and 6.5–32.5 hKDCs $\times 10^3$/cm^2 were seeded in REGM. In all experiments, medium was replaced every 2–3 days and all seeded scaffolds were cultured at 37°C in a 5% CO_2 atmosphere.

Cytological and histological staining

Bouin's-fixed, paraffin-embedded samples were stained with hematoxylin and eosin (H&E) or alcian blue pH 2.5 using standard procedures.[39] For immunochemical analyses, the peroxide-based EnVision technique was applied as previously described.[39] Primary antibodies [aquaporin-1 (1:1000, #ab9566; Abcam, Cambridge, United Kingdom), aquaporin-2 (1:300, #15081; Abcam), claudin-2 (1:200, #ab15100; Abcam), Col IV (1:25, #M0785; Dako, Hamburg, Germany), E-cadherin (1:300, #610181; BD Biosciences, Heidelberg, Germany), Ki67 (1:150, #M7240; Dako), mitochondria (1:250, #ab3298; Abcam), Na-K-ATPase (1:100, #ab76020; Abcam) and N-cadherin (1:300, #ab12221; Abcam)] were incubated in background-reducing antibody diluent (#S3022; Dako). For detection, peroxidase-conjugated EnVision reagents (#K4001 and #K4002; Dako) and diaminobenzidine chromogen (#K3468; Dako) were used. Samples were counterstained with hematoxylin.

For lectin staining, samples were treated with hydrogen peroxidase, and biotinylated *Lotus tetragonobolus* lectin (LTL, 1:500, #B1325; Biozol, Esching, Germany) or *Dolichos biflorus* agglutinin (DBA, 1:500, #B1035; Biozol) were prepared with background-reducing antibody diluent (#S3022; Dako). Detection included labeling with streptavidin (#LP000-ULE; DCS, Hamburg, Germany) and the addition of aminoethyl carbazole chromogen (#HK129-5KE; DCS). Sections were counterstained with hematoxylin.

To semi-quantify marker expression patterns, six images of each staining were counted. Hematoxylin staining was used to define cell nuclei and thus count cell numbers. Cells that were specifically stained by antibodies or lectins were normalized based on total cell numbers. All data are displayed as mean ± standard deviation. Statistical significance was assessed by a nonpaired Student's *t*-test. *p*-Values less than 0.05 were considered to be statistically significant.

Albumin uptake assay

To assess albumin uptake, the hKDC-seeded SIS was first preincubated in serum-free REGM for 1 h. The medium was then replaced by REGM containing 200 µg/mL fluorescein isothiocyanate-labeled bovine serum (BSA-FITC) (#A9771; Sigma-Aldrich, St. Louis, MO) and incubated for 30 min. The samples were then washed with PBS, counterstained with diamidino-2-phenylindole (DAPI), and imaged on a confocal laser scanning microscope (LSM 710; Zeiss, Oberkochen, Germany). DAPI staining was used to identify cell nuclei and thus assess cell numbers for semi-quantitative analysis. Cells that took up BSA-FITC were normalized based on total cell numbers. Data are displayed as mean ± standard deviation.

Scanning electron microscopy

Scanning electron microscopy (SEM) was performed on 3 µm paraffin sections. They were deparaffinized by incubation at 60°C for 30 and 10 min in xylene (#9713.3; Carl Roth), Roticlear (#A538.1; Carl Roth), and isopropanol (#10010401; Brenntag, Mülheim, Germany). Afterward, samples were air-dried, sputter coated with platinum, and micrographed using a scanning electron microscope (LEO 1530 VP; Zeiss, Oberkochen, Germany).

Results

hKDC characterization

Employing routine light microscopy, we observed that hKDCs at passage 4 showed a homogeneous epithelial morphology (Supplementary Fig. S1A; Supplementary Data are available online at www.liebertpub.com/tec). Cultures of hKDCs were analyzed for their ability to be expanded in culture. Cell populations were continually passaged for several weeks until senescence was reached. Senescence

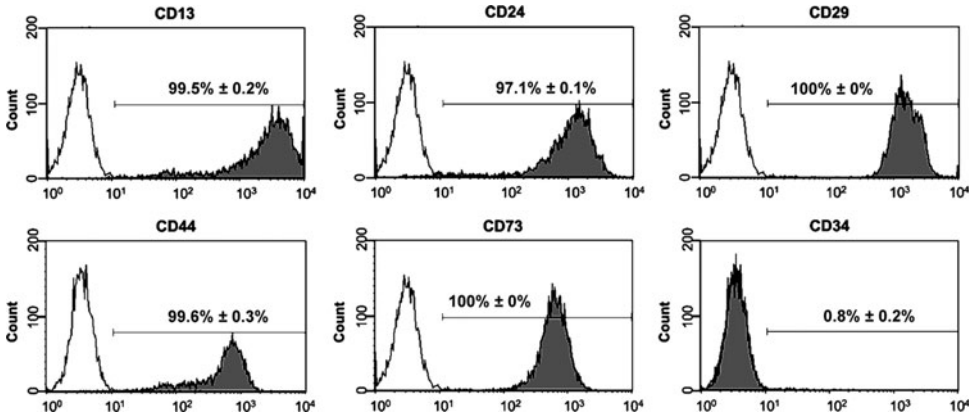

FIG. 1. Flow cytometry analysis of human kidney-derived cells (hKDCs). Histograms are displayed for cell surface markers CD13, CD24, CD29, CD44, CD73, and CD34 (gray) and corresponding isotype controls (white).

was determined when the cells failed to achieve greater than one population doubling during the study time interval. After 59 days in culture, hKDCs demonstrated 34 population doublings and were passaged 18 times. Cells demonstrated an average doubling time of 42 h per doubling (Supplementary Fig. S1B).

hKDCs were characterized by flow cytometry (Fig. 1). Similar to native PT cells *in vivo*, hKDCs expressed CD13 (99.5% ± 0.2%).[41] In addition, hKDCs also expressed CD24 (97.1% ± 0.1%), CD29 (100% ± 0%), CD44 (99.6% ± 0.3%), and CD73 (100% ± 0%), all surface markers that have been previously associated with renal progenitor cells and mesenchymal stem cells.[42–45] The vast majority of the hKDCs were negative for the hematopoietic stem cell marker CD34 (0.8% ± 0.2%). To further characterize hKDCs, we compared the presence of markers of PT cells (N-cadherin,[46] aquaporin-1[47]) and later nephron segments (E-cadherin,[46] aquaporin-2[47]) by immunocytological staining on hKDCs seeded in chamber slides (Fig. 2). In our study, N-cadherin was highly expressed in 100% ± 0% of the isolated hKDCs, whereas E-cadherin was detected only in 44.2% ± 3.0% of the cells (Fig. 2A vs. B). Aquaporin-1 was expressed by 1.0% ± 1.2% of the cells, while aquaporin-2 was not detectable (Fig. 2C vs. D). To detect proximally differentiated cells, LTL and DBA staining were used. LTL binds to carbohydrates of PT cells and DBA binds to later tubule segments.[48,49] We identified that LTL bound to 27.6% ± 5.2% of the hKDCs (Fig. 2E). In contrast, DBA bound only to 7.1% ± 1.7% of the hKDCs (Fig. 2F).

Growth patterns of hKDCs under routine culture conditions

hKDC growth patterns were studied in setups that are currently used as *in vitro* models of the renal epithelium. The most basic model represents cells cultured in routine polystyrene cell culture plates (Fig. 3A). After achieving confluence, hKDCs continued to proliferate on this substrate, leading to uncontrollable cellular overgrowth and formation of 3D cell aggregates that partially detached from the culture substrate.[17] In contrast, it has been shown that porous well inserts allow a compartmentalization and are therefore suitable for transport studies.[20] Therefore, we seeded hKDCs on Col I-coated PET membrane inserts. The cells showed a flat, noncuboidal morphology, similar to what had been seen on cell culture polystyrene (Fig. 3B). Further, hKDCs did not form a single cell layer, but grew in multiple layers. Cell agglomerates formed that frequently detached, suggesting poor adherence on the Col I-coated PET membrane (Fig. 3B). In previous studies, hydrogels composed of Col I were used due to their ability to induce cyst and tubule formation, while allowing a normal epithelial morphogenesis of RPTECs.[17] In this study, hKDCs grown on Col I-3D-gels formed cystic and tubule structures and displayed a typical

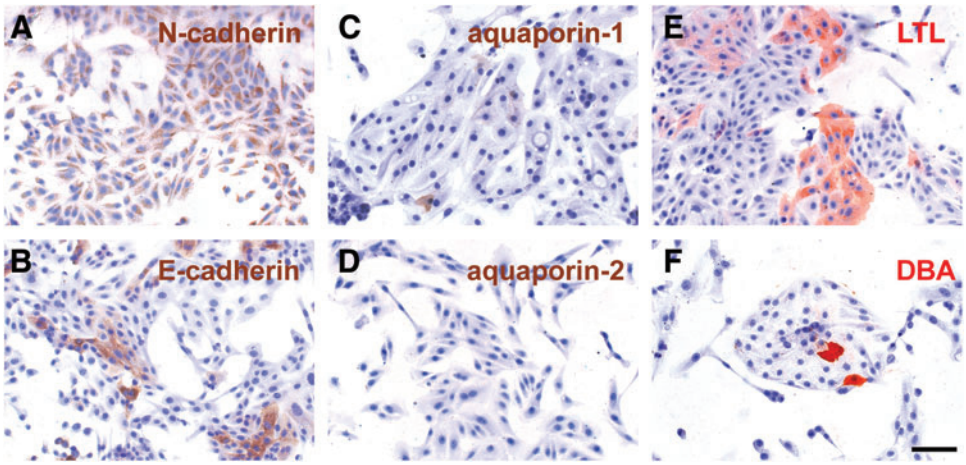

FIG. 2. Immunocytological analyses of hKDCs utilizing N-cadherin **(A)**, E-cadherin **(B)** aquaporin-1 **(C)**, aquaporin-2 **(D)**, *Lotus tetragonobolus* lectin (LTL) **(E)**, and *Dolichos biflorus* agglutinin (DBA) **(F)**. **(A–D)** Antigens are depicted in brown; **(E, F)** carbohydrates are displayed in red. Nuclei are counterstained with hematoxylin (blue). Scale bar = 100 µm. Color images available online at www.liebertpub.com/tec

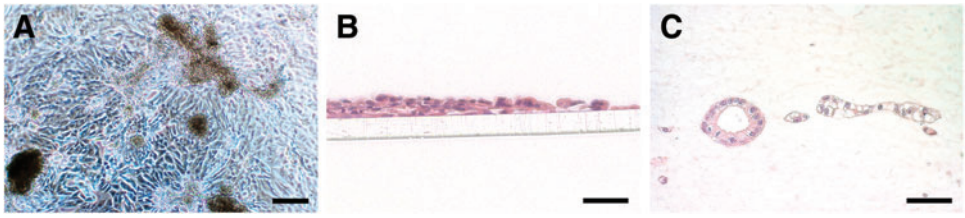

FIG. 3. **(A)** Bright-field image of hKDCs that were cultured on a routine polystyrene substrate. Scale bar = 200 µm. **(B, C)** Hematoxylin and eosin (H&E) staining of hKDCs cultured on collagen type I (Col I)-coated polyethylene terephthalate membranes **(B)** or hKDCs grown on Col I-3D-gels **(C)**. Scale bars = 50 µm. Color images available online at www.liebertpub.com/tec

epithelial morphology, confirming the tubulogenic potential of the cells (Fig. 3C); however, tubule structures were diffusely distributed within the gel. Thus, transport studies with defined substance addition and detection in apical and basal compartments are not feasible in this model.

Impact of SIS scaffold on hKDC and HK-2 cell growth and morphology

SIS was used to combine the promoting effect of a natural 3D scaffold on epithelial cell morphology with a surface that allows a planar monolayer culture. hKDCs were cultured on the SIS for 3 weeks and then analyzed by histological and immunohistological staining (Fig. 4). The cells formed an epithelial monolayer with a cuboidal to high-prismatic morphology and eccentric nuclei, which is very similar to the morphology of PT cells *in vivo*. In contrast to hKDCs that were cultured on Col I-coated PET membrane inserts, hKDCs cultured on SIS did not overgrow and formed a single epithelial cell layer, analogous to the morphology of native kidney tissue (Fig. 4B vs. C). Ki67 staining revealed that similar to the Ki67 patterns in native tissue, very few proliferating cells were present in the hKDC-SIS cultures after 3 weeks, further demonstrating contact inhibition of hKDCs on the SIS (Fig. 4D, E).

HK-2 cells represent a PT epithelial cell line of human origin.[39] These cells are routinely used for *in vitro* studies.[50,51] Here, we compared growth patterns of hKDCs with HK-2 cells cultured on the SIS. We observed extensive proliferation and multilayer formation of HK-2 cells on the SIS (Fig. 4F, G). After 3 weeks, proliferating cells were detected in all cell layers. Moreover, histological results indicated cell degradation (Fig. 4F; arrows). In contrast to HK-2 cells, hKDCs exhibited more epithelial cell characteristics under the described culture

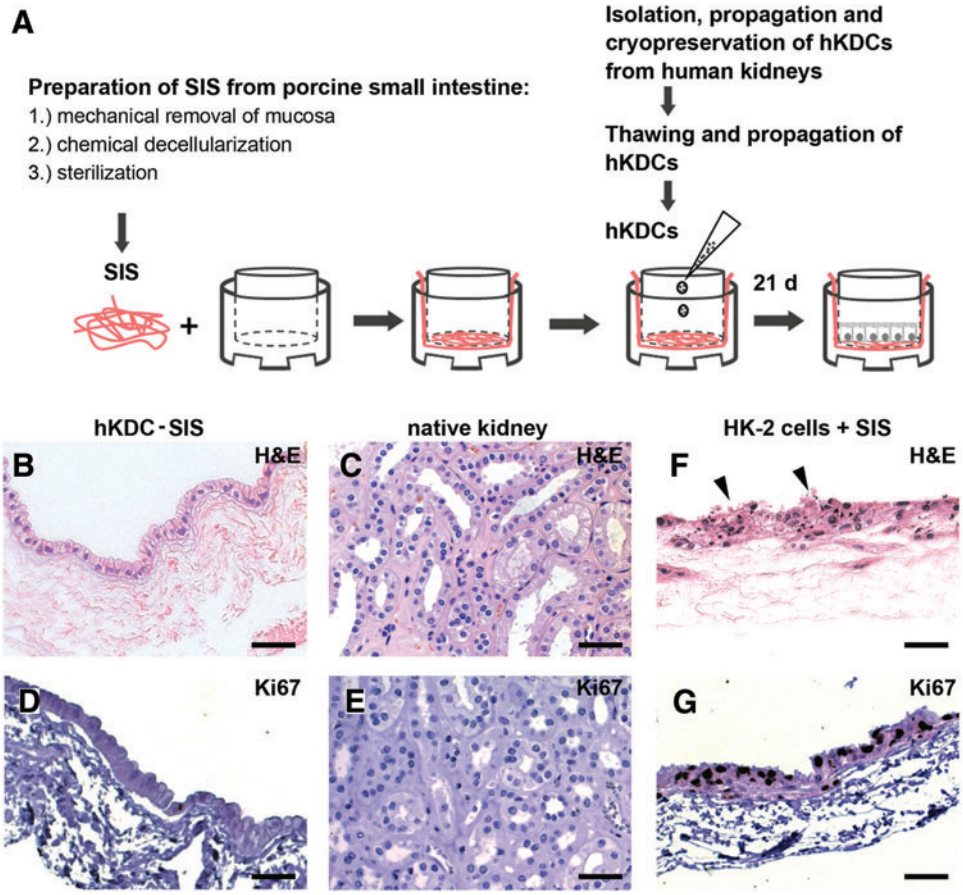

FIG. 4. **(A)** Schematic depiction of the procedure used to establish the hKDC-small intestinal submucosa (SIS) *in vitro* culture model. **(B, C, F)** H&E staining of hKDC-SIS cultures **(B)**, native kidney tissue **(C)**, and HK-2 cells grown on SIS **(F)**. **(D, E, G)** Ki67 immunohistochemistry (dark brown) revealed that in contrast to the hKDC-SIS constructs **(D)** and native kidney tissue **(E)**, HK-2 cells were highly proliferative and cell degradation (arrows) was observed **(G)**. Cell nuclei were counterstained with hematoxylin (blue). All scale bars = 50 µm. Color images available online at www.liebertpub.com/tec

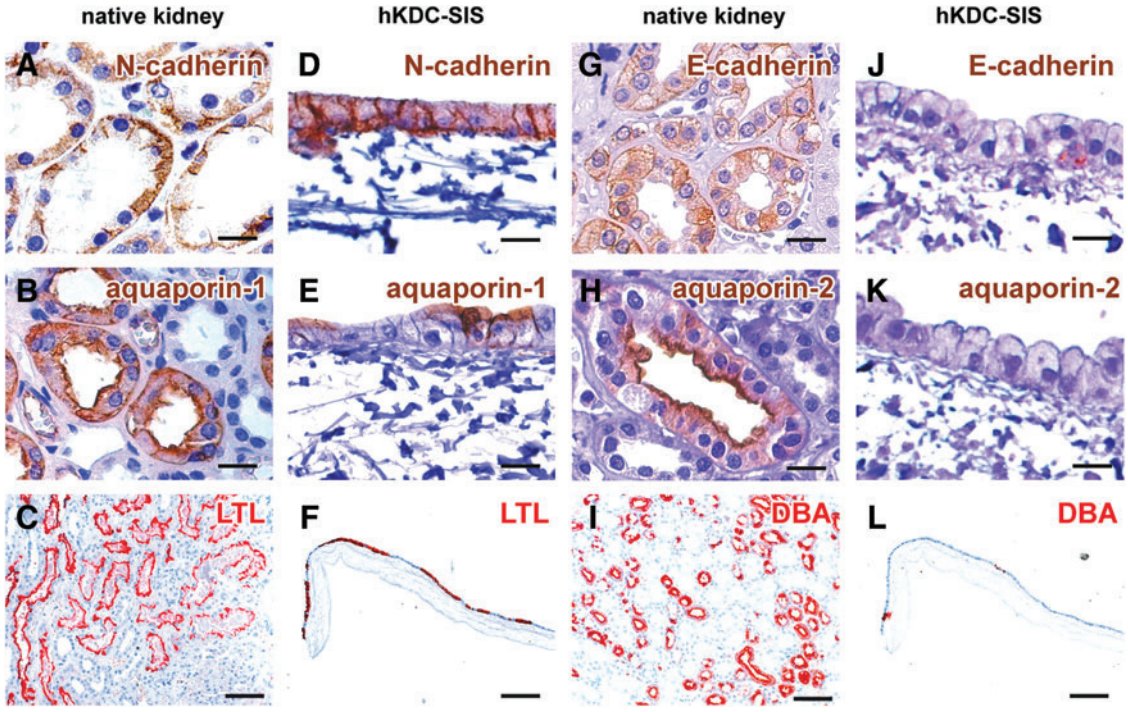

FIG. 5. Immunohistochemical and lectin staining of native kidney tissue **(A–C** and **G–I)** compared to hKDCs cultured on SIS for 21 days **(D–F** and **J–L)**. We analyzed markers of the proximal tubule including N-cadherin (brown**; A, D)** and aquaporin-1 (brown**; B, E)**, and LTL (red**; C, F)**. Staining is also provided for markers of later nephron segments including E-cadherin (brown**; G, J)**, aquaporin-2 (brown**; H, K)**, and DBA (red**; I, L)**. Nuclei were counterstained with hematoxylin (blue). Scale bars: **(A, B, D, E, G, H, J, K)** = 20 μm, **(C, F, I, L)** = 200 μm. Color images available online at www.liebertpub.com/tec

conditions and were therefore selected for all ongoing experiments (Fig. 4B, D vs. F, G).

Cell phenotypical characterization of hKDCs on the SIS

We analyzed expression patterns of markers that are present in native renal PT cells (Fig. 5A–C) and later nephron segments (Fig. 5G–I) to further characterize hKDCs on the SIS. We identified that N-cadherin was expressed in 100% ± 0% of the hKDCs on the SIS (Fig. 5D). Aquaporin-1 was detected in 38.2% ± 4.7% of the SIS-cultured hKDCs, particularly on the apical cell membrane, indicating cellular polarization (Fig. 5E). We further showed that 45.4% ± 7.1% of the hKDCs on SIS were positive for LTL (Fig. 5F), which represents a significant increase of

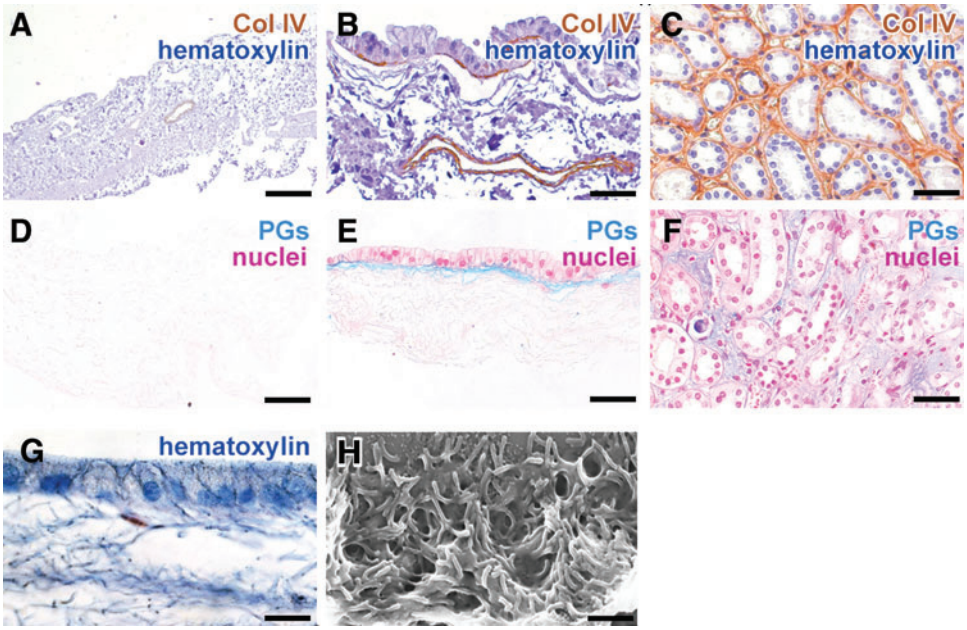

FIG. 6. **(A–F)** Acellular SIS **(A, D)**, hKDCs cultured on SIS for 21 days **(B, E)**, and native kidney tissue **(C, F)** are stained for collagen type IV (Col IV) **(A–C;** brown, nuclei are counterstained with hematoxylin [blue]) and alcian blue (pH 2.5) **(D–F;** proteoglycans [PGs] in blue, nuclei are counterstained with nuclear fast red). **(G, H)** In hKDCs-SIS cultures, microvilli formation is visualized using hematoxylin **(G)** and via scanning electron microscopy (SEM) **(H)**. Scale bars **(A)** = 200 μm, **(B, C, E, F)** = 50 μm, **(G)** = 20 μm, **(H)** = 1 μm. Color images available online at www.liebertpub.com/tec

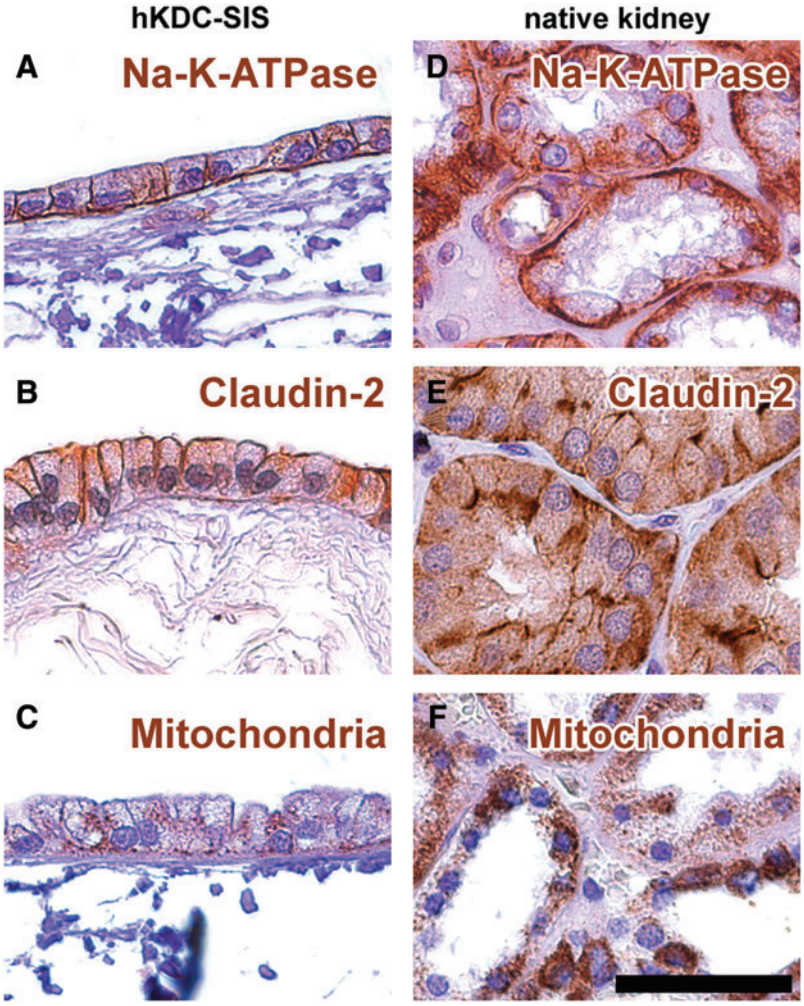

FIG. 7. Immunohistochemical staining of **(A–C)** hKDCs cultured on SIS for 21 days and **(D–F)** native kidney tissue. Antigens are depicted in brown: **(A, D)** Na-K-ATPase, **(B, E)** claudin-2, and **(C, F)** mitochondria. Cell nuclei were counterstained with hematoxylin (blue). The scale bar = 50 μm. Color images available online at www.liebertpub.com/tec

LTL expression when compared with hKDCs before exposure to the 3D substrate (Fig. 2E). In contrast, E-cadherin was only seen in 17.3% ± 3.4% of the cells (Fig. 5J), and no positive staining of aquaporin-2 was observed at any time of *in vitro* culture (Fig. 5K). Only 8.4% ± 2.0% of the cells were positive for DBA (Fig. 5L).

The basement membrane protein Col IV and proteoglycans were detected underneath the basal cell membrane of hKDCs, but not on the surface of the acellular scaffold, indicating a neo-synthesis of crucial ECM proteins by the hKDCs (Fig. 6A–F). On the apical cell membrane, microvilli structures were observed in histological stains, which were confirmed by SEM (Fig. 6G, H). Strong basolateral expression of Na-K-ATPase (Fig. 7A), expression of the tight junctional protein claudin-2 (Fig. 7B), and basal accumulation of mitochondria (Fig. 7C) further confirmed the formation of a polarized monolayer.

In the healthy kidney, the albumin filtration rate is very low, but in renal disease it can increase. In both instances, albumin needs to be recovered by PT cells. Accordingly, we

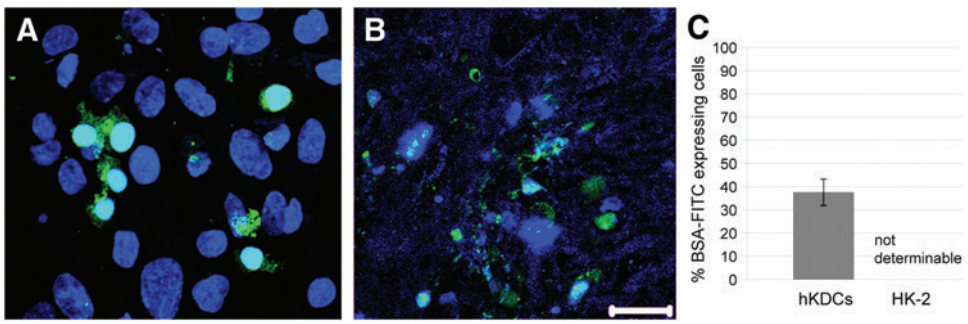

FIG. 8. Fluorescein isothiocyanate-labeled bovine serum (BSA-FITC) uptake assay. **(A)** hKDCs cultured on the SIS for 21 days take up BSA-FITC. **(B)** With HK-2 cells cultured on the SIS for 21 days, only fragments of nuclei and BSA-FITC could be observed. **(C)** Quantitative analysis, $n = 3$. **(A, B)** Diamidino-2-phenylindole (DAPI) = blue, BSA-FITC = green. Scale bar = 20 μm. Color images available online at www.liebertpub.com/tec

analyzed the albumin uptake of hKDCs on the SIS and revealed that 37.7% ± 5.7% of hKDCs on the SIS were able to uptake BSA-FITC. For HK-2 cells on the SIS only fragments of BSA-FITC and DAPI counterstaining could be observed and thus quantification of the staining was not possible (Fig. 8).

Discussion

Human *in vitro*-manufactured tissue and organ models are powerful enabling tools for the exploration of fundamental questions regarding cell, matrix, and developmental biology in addition to the study of drug delivery dynamics and kinetics, provided that a suitable combination of cells, scaffolds, and culture conditions is available.[52] The establishment of a fully functional human-based renal PT *in vitro* test system would be of great interest to the fields of physiological science, pharmacological research, and BAK development, where cell-scaffold composites mimicking *in vivo* tissue elements are urgently required.[7] Three-dimensional scaffolds play an important role in the appropriate growth and differentiation of epithelial cells *ex vivo*, with natural ECM representing a suitable substrate to support cell-typical characteristics.[53]

In our study, we used the combination of primary isolated hKDCs with SIS to mimic the human renal PT. Initially, hKDCs were isolated and characterized in regard to their morphology, growth potential, and marker expression. hKDCs performed 34 population doublings until senescence, which shows that high quantities of cells can be generated. hKDCs express the surface markers CD13, CD24, CD29, CD44, and CD73. This marker profile suggests that hKDCs are a renal progenitor cell-like population; however, it was shown by Metsuyanim *et al.* that CD24 can be also found on a high amount of cells in adult human kidney tissue.[42]

ECM proteins that can help to mimic the native organ's microenvironment have been shown to be beneficial when establishing *in vitro* cultures and test systems.[9] It has been shown that collagen types I and IV, and laminins supported culture of human RPTECs.[11] Col I is a natural constituent of the kidney,[54,55] and it has been previously described as an appropriate substrate for the culture of PT cells on membranes.[56] Here, we cultured hKDCs on routine cell culture polystyrene, Col I-coated PET membrane inserts, and on Col I-3D-gels to evaluate the potential of these cells for their use in a renal PT *in vitro* model. We demonstrated that hKDCs that were cultured on routine polystyrene cell culture plates or synthetic Col I-coated PET membranes did not develop physiological morphologies and grew in multiple layers, which leads to the conclusion that they had lost contact inhibition. In contrast, when cultured in a Col I-3D-gel, hKDCs differentiated into cystic and tubule epithelial structures. One difference between the Col I-coated PET membrane cultures and the Col I-3D-gels was three-dimensionality. These results imply that using appropriate ECM components alone might be insufficient to induce epithelial characteristics of hKDCs and that three-dimensionality is required to obtain a physiological resemblance of these cells *in vitro*, a phenomenon that has been previously described by others.[18] Further parameters that may also have influenced the results in our experimental setup could be differences in the bulk modulus[57,58] between the Col I gel and the Col I-coated PET membrane, or different diffusion rates of nutrients, growth factors, and paracrine signals.[59] However, transport studies and BAK designs require the assembly of a planar epithelial cell layer. Our data suggest that Col I-coated synthetic PET membranes are not suitable for achieving planar cell assembly, since cultures employing hKDCs showed a lack of contact inhibition and therefore pathological cell proliferation patterns.

We identified SIS as suitable substrate to support formation of an epithelial monolayer since this natural ECM scaffold features a variety of biochemical and structural properties that stimulate cell adhesion and differentiation.[31] In our experiments, culture of hKDCs on SIS led to the formation of a contact-inhibited monolayer. We also included HK-2 cells in our experimental design, since it is a cell line derived from normal adult human kidney tissue; however, due to its transformation with human papillomavirus type 16 E6/E7 genes, the cells lack normal contact inhibition. Thus, no epithelial monolayer could be achieved on the SIS using the HK-2 cells. Implementation of a BSA-FITC assay revealed an increased HK-2 cell degradation reflected by highly fragmented staining. We hypothesize that the observed HK-2 cell degradation might be the result of fast consumption of nutrients in the medium caused by a high cell proliferation rate. This emphasizes that transformed cell lines might not be an adequate cell source for *in vitro* test systems.

For the evaluation of proximal differentiation, we analyzed the hKDC-SIS cultures for N-cadherin and aquaporin-1, which are both expressed in RPTECs of the native kidney tissue. We additionally stained for E-cadherin and aquaporin-2, which are found in epithelial cells of later tubule segments. In our system, a strong continuing expression of N-cadherin throughout the entire culture period was observed. Aquaporin-1 expression significantly increased on the SIS when compared with hKDCs grown on routine polystyrene culture plates; however, overall expression of this marker was lower in the hKDC-SIS cultures when compared with the PTs of the native human kidney tissue. In contrast, aquaporin-2 was not expressed in the hKDC-SIS cultures. When cultured on SIS, more than double of the hKDCs were positive for LTL staining when compared with hKDCs cultured on routine polystyrene. DBA staining before and after hKDC culture on the SIS did not show significant differences. These results indicate that although there are some differences between the 3D hKDC-SIS culture model and native human kidney tissue, hKDC culture on SIS leads to an increased expression of renal PT-associated markers and a decrease of markers that are associated with later tubule segments and thus supports proximal differentiation. However, not all cells expressed all PT markers, which can be due to either dedifferentiation or incomplete differentiation.

Col IV is the most abundant collagen of the renal tubule basement membrane.[60] Interestingly, we detected no Col IV expression in the acellular SIS prior cell seeding; however, a robust Col IV expression was seen underneath the hKDC cells when cultured on the SIS substrate, which indicates normal Col IV synthesis and directed basal deposition by the hKDCs. This process was previously associated with regeneration of the tubule epithelium after sublethal injury.[61] Other data suggested that hKDCs synthesize Col IV to allow the formation of a polarized epithelium, similar to the

regenerative processes seen *in vivo*.[61] The synthesis of Col IV on SIS has been previously shown for epidermal cells,[33] which highlights the supporting influence of SIS for the formation of epithelial structures *in vitro*. The superiority of SIS as 3D culture substrate for hKDCs over routine porous PET membrane inserts was further supported by our observation that hKDCs cultured on Col I-coated PET membranes formed detaching cell aggregates. Physiological cell polarization and microvilli formation could only be observed in the hKDC-SIS cultures. Polarization was further confirmed by Na-K-ATPase, claudin-2, and mitochondria staining.

In summary, our study is the first to culture renal cells on SIS. We showed that SIS highly promotes the formation of an epithelial monolayer from hKDCs, which was neither achieved on routine tissue culture polystyrene culture ware nor on Col I-coated PET membranes. Interestingly, HK-2 cells were not receptive to the promoting influence of the natural ECM, most likely due to their viral transformation. This corresponds with a study of Wang *et al.* that showed that growth and apoptosis of normal, but not transformed cells, is regulated by substrate characteristics.[62] In contrast, primary isolated hKDCs proved to be a very useful cell source when aiming toward the establishment of a renal PT *in vitro* model. These cells could be expanded to high passages until senescence, without losing their phenotypical characteristics. Moreover, hKDCs developed a single polarized epithelial cell layer on the SIS. Future research efforts will focus on clarifying the parameters that are responsible for the partly inhomogeneous hKDC morphology and differentiation, which could be due to the cells themselves, the scaffold material, or both.

Conclusion

In this study, we cultured primary isolated hKDCs on conventional *in vitro* substrates such as porous membrane inserts and Col I-3D-gels. In addition, we used SIS as substrate material, which is generally well known for its supportive impact on cellular ingrowth and differentiation, but had not been used for the culture of renal tubule cells. Our results demonstrate that SIS supports the formation of a single cell layer with characteristics of the natural renal proximal epithelium when using hKDCs, but not virally immortalized HK-2 cells. We conclude that the combination of hKDCs and SIS is a suitable cell-scaffold composite to mimic the human renal PT *in vitro*. In further experiments, we will investigate transport capacity and sensitivity to nephrotoxic substances in the culture model to demonstrate that epithelial morphology and polarization enables cell functionality, which would qualify this model as complement or alternative to animal testing.

Acknowledgments

We thank Dominique Tordy for explanting the porcine small intestine, Jasmin Kuttner for her technical support, and Shannon Lee Layland for his helpful comments on the article (all Fraunhofer IGB Stuttgart). The authors are grateful for the financial support by Advanced Technologies & Regenerative Medicine, LLC* (On December 30, 2012, ATRM merged into DePuy Orthopaedics, Inc.), the Fraunhofer-Gesellschaft and the Ministry of Science, Research, and the Arts of Baden-Württemberg (33-729.55-3/214 to K.S.L.).

Disclosure Statement

The following authors have an employment position to disclose: David Colter holds a full-time employment with Janssen Research & Development, LLC, Janssen Pharmaceutical Companies of Johnson & Johnson, an affiliate of an entity having a commercial interest in the subject matter under consideration in the article. Christian Kazanecki holds a full-time employment with Janssen Diagnostics, Inc., an affiliate of an entity having a commercial interest in the subject matter under consideration in the article. Anna Gosiewska holds a full-time employment with Johnson & Johnson Consumer and Personal Products Worldwide, an affiliate of an entity having a commercial interest in the subject matter under consideration in the article. Name of entities having a commercial interest: DePuy Synthes Products, LLC, and Janssen Biotech, Inc.

References

1. Wagner, M.C., and Molitoris, B.A. Renal epithelial polarity in health and disease. Pediatr Nephrol **13,** 163, 1999.
2. Lock, E.A., and Reed, C.J. Xenobiotic metabolizing enzymes of the kidney. Toxicol Pathol **26,** 18, 1998.
3. Launay-Vacher, V., Izzedine, H., Karie, S., Hulot, J.S., Baumelou, A., and Deray, G. Renal tubular drug transporters. Nephron Physiol **103,** 97, 2006.
4. Humes, H.D., MacKay, S.M., Funke, A.J., and Buffington, D.A. Tissue engineering of a bioartificial renal tubule assist device: *in vitro* transport and metabolic characteristics. Kidney Int **55,** 2502, 1999.
5. Ding, F., and Humes, H.D. The bioartificial kidney and bioengineered membranes in acute kidney injury. Nephron Exp Nephrol **109,** e118, 2008.
6. Tasnim, F., Deng, R., Hu, M., Liour, S., Li, Y., Ni, M., Ying, J.Y., and Zink, D. Achievements and challenges in bioartificial kidney development. Fibrogenesis Tissue Repair **3,** 14, 2010.
7. Oo, Z.Y., Deng, R., Hu, M., Ni, M., Kandasamy, K., Bin Ibrahim, M.S., Ying, J.Y., and Zink, D. The performance of primary human renal cells in hollow fiber bioreactors for bioartificial kidneys. Biomaterials **32,** 8806, 2011.
8. Pampaloni, F., Reynaud, E.G., and Stelzer, E.H. The third dimension bridges the gap between cell culture and live tissue. Nat Rev Mol Cell Biol **8,** 839, 2007.
9. Hinderer, S., Schesny, M., Bayrak, A., Ibold, B., Hampel, M., Walles, T., Stock, U.A., Seifert, M., and Schenke-Layland, K. Engineering of fibrillar decorin matrices for a tissue-engineered trachea. Biomaterials **33,** 5259, 2012.
10. Votteler, M., Kluger, P.J., Walles, H., and Schenke-Layland, K. Stem cell microenvironments—unveiling the secret of how stem cell fate is defined. Macromol Biosci **10,** 1302, 2010.
11. Zhang, H., Tasnim, F., Ying, J.Y., and Zink, D. The impact of extracellular matrix coatings on the performance of human renal cells applied in bioartificial kidneys. Biomaterials **30,** 2899, 2009.
12. Ni, M., Teo, J.C., Ibrahim, M.S., Zhang, K., Tasnim, F., Chow, P.Y., Zink, D., and Ying, J.Y. Characterization of membrane materials and membrane coatings for bioreactor units of bioartificial kidneys. Biomaterials **32,** 1465, 2011.

13. Kanai, N., Fujita, Y., Kakuta, T., and Saito, A. The effects of various extracellular matrices on renal cell attachment to polymer surfaces during the development of bioartificial renal tubules. Artif Organs **23,** 114, 1999.
14. Hall, H.G., Farson, D.A., and Bissell, M.J. Lumen formation by epithelial cell lines in response to collagen overlay: a morphogenetic model in culture. Proc Natl Acad Sci U S A **79,** 4672, 1982.
15. Wang, A.Z., Ojakian, G.K., and Nelson, W.J. Steps in the morphogenesis of a polarized epithelium. I. Uncoupling the roles of cell-cell and cell-substratum contact in establishing plasma membrane polarity in multicellular epithelial (MDCK) cysts. J Cell Sci **95(Pt 1),** 137, 1990.
16. O'Brien, L.E., Zegers, M.M., and Mostov, K.E. Opinion: Building epithelial architecture: insights from three-dimensional culture models. Nat Rev Mol Cell Biol **3,** 531, 2002.
17. Chung, I.M., Enemchukwu, N.O., Khaja, S.D., Murthy, N., Mantalaris, A., and Garcia, A.J. Bioadhesive hydrogel microenvironments to modulate epithelial morphogenesis. Biomaterials **29,** 2637, 2008.
18. Guo, Q., Xia, B., Moshiach, S., Xu, C., Jiang, Y., Chen, Y., Sun, Y., Lahti, J.M., and Zhang, X.A. The microenvironmental determinants for kidney epithelial cyst morphogenesis. Eur J Cell Biol **87,** 251, 2008.
19. Astashkina, A.I., Mann, B.K., Prestwich, G.D., and Grainger, D.W. A 3-D organoid kidney culture model engineered for high-throughput nephrotoxicity assays. Biomaterials **33,** 4700, 2012.
20. Justice, B.A., Badr, N.A., and Felder, R.A. 3D cell culture opens new dimensions in cell-based assays. Drug Discov Today **14,** 102, 2009.
21. Badylak, S.F., Record, R., Lindberg, K., Hodde, J., and Park, K. Small intestinal submucosa: a substrate for *in vitro* cell growth. J Biomater Sci Polym Ed **9,** 863, 1998.
22. Badylak, S.F., Freytes, D.O., and Gilbert, T.W. Extracellular matrix as a biological scaffold material: structure and function. Acta Biomater **5,** 1, 2009.
23. Badylak, S.F. Small-intestinal submucosa (SIS): a biomaterial conducive to smart tissue remodeling. In: Bell, E., ed. *Tissue Engineering: Current Perspectives*. Boston, MA: Birkhäuser, 1993, pp. 179–189.
24. Hodde, J., and Hiles, M. Constructive soft tissue remodelling with a biologic extracellular matrix graft: overview and review of the clinical literature. Acta Chir Belg **107,** 641, 2007.
25. Santucci, R.A., and Barber, T.D. Resorbable extracellular matrix grafts in urologic reconstruction. Int Braz J Urol **31,** 192, 2005.
26. Hodde, J.P., Badylak, S.F., Brightman, A.O., and Voytik-Harbin, S.L. Glycosaminoglycan content of small intestinal submucosa: a bioscaffold for tissue replacement. Tissue Eng **2,** 209, 1996.
27. Voytik-Harbin, S.L., Brightman, A.O., Kraine, M.R., Waisner, B., and Badylak, S.F. Identification of extractable growth factors from small intestinal submucosa. J Cell Biochem **67,** 478, 1997.
28. Hodde, J.P., Record, R.D., Liang, H.A., and Badylak, S.F. Vascular endothelial growth factor in porcine-derived extracellular matrix. Endothelium **8,** 11, 2001.
29. McDevitt, C.A., Wildey, G.M., and Cutrone, R.M. Transforming growth factor-beta1 in a sterilized tissue derived from the pig small intestine submucosa. J Biomed Mater Res A **67,** 637, 2003.
30. Hodde, J., Janis, A., and Hiles, M. Effects of sterilization on an extracellular matrix scaffold: part II. Bioactivity and matrix interaction. J Mater Sci Mater Med **18,** 545, 2007.
31. Brown-Etris, M., Cutshall, W.D., and Hiles, M.C. A new biomaterial derived from small intestine submucosa and developed into a wound matrix device. Wounds **14,** 150, 2002.
32. Voytik-Harbin, S.L., Brightman, A.O., Waisner, B.Z., Robinson, J.P., and Lamar, C.H. Small intestinal submucosa: a tissue-derived extracellular matrix that promotes tissue-specific growth and differentiation of cells *in vitro*. Tissue Eng **4,** 157, 1998.
33. Lindberg, K., and Badylak, S.F. Porcine small intestinal submucosa (SIS): a bioscaffold supporting *in vitro* primary human epidermal cell differentiation and synthesis of basement membrane proteins. Burns **27,** 254, 2001.
34. Yang, B., Zhou, L., Sun, Z., Yang, R., Chen, Y., and Dai, Y. *In vitro* evaluation of the bioactive factors preserved in porcine small intestinal submucosa through cellular biological approaches. J Biomed Mater Res A **93,** 1100, 2010.
35. Gupta, S., and Rosenberg, M.E. Do stem cells exist in the adult kidney? Am J Nephrol **28,** 607, 2008.
36. Benigni, A., Morigi, M., and Remuzzi, G. Kidney regeneration. Lancet **375,** 1310, 2010.
37. Lindgren, D., Bostrom, A.K., Nilsson, K., Hansson, J., Sjolund, J., Moller, C., Jirstrom, K., Nilsson, E., Landberg, G., Axelson, H., and Johansson, M.E. Isolation and characterization of progenitor-like cells from human renal proximal tubules. Am J Pathol **178,** 828, 2011.
38. Sagrinati, C., Netti, G.S., Mazzinghi, B., Lazzeri, E., Liotta, F., Frosali, F., Ronconi, E., Meini, C., Gacci, M., Squecco, R., Carini, M., Gesualdo, L., Francini, F., Maggi, E., Annunziato, F., Lasagni, L., Serio, M., Romagnani, S., and Romagnani, P. Isolation and characterization of multipotent progenitor cells from the Bowman's capsule of adult human kidneys. J Am Soc Nephrol **17,** 2443, 2006.
39. Ryan, M.J., Johnson, G., Kirk, J., Fuerstenberg, S.M., Zager, R.A., and Torok-Storb, B. HK-2: an immortalized proximal tubule epithelial cell line from normal adult human kidney. Kidney Int **45,** 48, 1994.
40. Pusch, J., Votteler, M., Gohler, S., Engl, J., Hampel, M., Walles, H., and Schenke-Layland, K. The physiological performance of a three-dimensional model that mimics the microenvironment of the small intestine. Biomaterials **32,** 7469, 2011.
41. Kotlo, K., Shukla, S., Tawar, U., Skidgel, R.A., and Danziger, R.S. Aminopeptidase N reduces basolateral Na+-K+-ATPase in proximal tubule cells. Am J Physiol Renal Physiol **293,** F1047, 2007.
42. Metsuyanim, S., Harari-Steinberg, O., Buzhor, E., Omer, D., Pode-Shakked, N., Ben-Hur, H., Halperin, R., Schneider, D., and Dekel, B. Expression of stem cell markers in the human fetal kidney. PLoS One **4,** e6709, 2009.
43. Lazzeri, E., Crescioli, C., Ronconi, E., Mazzinghi, B., Sagrinati, C., Netti, G.S., Angelotti, M.L., Parente, E., Ballerini, L., Cosmi, L., Maggi, L., Gesualdo, L., Rotondi, M., Annunziato, F., Maggi, E., Lasagni, L., Serio, M., Romagnani, S., Vannelli, G.B., and Romagnani, P. Regenerative potential of embryonic renal multipotent progenitors in acute renal failure. J Am Soc Nephrol **18,** 3128, 2007.
44. Bussolati, B., Bruno, S., Grange, C., Buttiglieri, S., Deregibus, M.C., Cantino, D., and Camussi, G. Isolation of renal progenitor cells from adult human kidney. Am J Pathol **166,** 545, 2005.

45. Dominici, M., Le Blanc, K., Mueller, I., Slaper-Cortenbach, I., Marini, F., Krause, D., Deans, R., Keating, A., Prockop, D., and Horwitz, E. Minimal criteria for defining multipotent mesenchymal stromal cells. The International Society for Cellular Therapy position statement. Cytotherapy **8,** 315, 2006.
46. Prozialeck, W.C., and Edwards, J.R. Cell adhesion molecules in chemically-induced renal injury. Pharmacol Ther **114,** 74, 2007.
47. Nielsen, S., Frokiaer, J., Marples, D., Kwon, T.H., Agre, P., and Knepper, M.A. Aquaporins in the kidney: from molecules to medicine. Physiol Rev **82,** 205, 2002.
48. Hennigar, R.A., Schulte, B.A., and Spicer, S.S. Heterogeneous distribution of glycoconjugates in human kidney tubules. Anat Rec **211,** 376, 1985.
49. Truong, L.D., Phung, V.T., Yoshikawa, Y., and Mattioli, C.A. Glycoconjugates in normal human kidney. A histochemical study using 13 biotinylated lectins. Histochemistry **90,** 51, 1988.
50. Wang, Y.F., Shyu, H.W., Chang, Y.C., Tseng, W.C., Huang, Y.L., Lin, K.H., Chou, M.C., Liu, H.L., and Chen, C.Y. Nickel (II)-induced cytotoxicity and apoptosis in human proximal tubule cells through a ROS- and mitochondria-mediated pathway. Toxicol Appl Pharmacol **259,** 177, 2012.
51. Gunness, P., Aleksa, K., Kosuge, K., Ito, S., and Koren, G. Comparison of the novel HK-2 human renal proximal tubular cell line with the standard LLC-PK1 cell line in studying drug-induced nephrotoxicity. Can J Physiol Pharmacol **88,** 448, 2010.
52. Schenke-Layland, K., and Nerem, R.M. *In vitro* human tissue models—moving towards personalized regenerative medicine. Adv Drug Deliv Rev **63,** 195, 2011.
53. Schenke-Layland, K., Nsair, A., Van Handel, B., Angelis, E., Gluck, J.M., Votteler, M., Goldhaber, J.I., Mikkola, H.K., Kahn, M., and Maclellan, W.R. Recapitulation of the embryonic cardiovascular progenitor cell niche. Biomaterials **32,** 2748, 2011.
54. Alexakis, C., Maxwell, P., and Bou-Gharios, G. Organ-specific collagen expression: implications for renal disease. Nephron Exp Nephrol **102,** e71, 2006.
55. Yoshioka, K., Tohda, M., Takemura, T., Akano, N., Matsubara, K., Ooshima, A., and Maki, S. Distribution of type I collagen in human kidney diseases in comparison with type III collagen. J Pathol **162,** 1990.
56. Terryn, S., Jouret, F., Vandenabeele, F., Smolders, I., Moreels, M., Devuyst, O., Steels, P., and Van Kerkhove, E. A primary culture of mouse proximal tubular cells, established on collagen-coated membranes. Am J Physiol Renal Physiol **293,** 2007.
57. Discher, D.E., Janmey, P., and Wang, Y.L. Tissue cells feel and respond to the stiffness of their substrate. Science **310,** 1139, 2005.
58. Ladoux, B., and Nicolas, A. Physically based principles of cell adhesion mechanosensitivity in tissues. Rep Prog Phys **75,** 116601, 2012.
59. Baker, B.M., and Chen, C.S. Deconstructing the third dimension: how 3D culture microenvironments alter cellular cues. J Cell Sci **125(Pt 13),** 3015, 2012.
60. Miner, J.H. Renal basement membrane components. Kidney Int **56,** 2016, 1999.
61. Nony, P.A., Nowak, G., and Schnellmann, R.G. Collagen IV promotes repair of renal cell physiological functions after toxicant injury. Am J Physiol Renal Physiol **281,** F443, 2001.
62. Wang, H.B., Dembo, M., and Wang, Y.L. Substrate flexibility regulates growth and apoptosis of normal but not transformed cells. Am J Physiol Cell Physiol **279,** C1345, 2000.

Address correspondence to:
Katja Schenke-Layland, PhD, MSc
Department of Cell and Tissue Engineering
Fraunhofer Institute for Interfacial
Engineering and Biotechnology (IGB)
Nobelstr. 12
Stuttgart 70569
Germany

E-mail: katja.schenke-layland@igb.fraunhofer.de

Received: July 24, 2013
Accepted: November 13, 2013
Online Publication Date: January 2, 2014